Karlsruhe Institute of Technology

Visualization of Lithosphere Subduction: Application to the Mantle Evolution beneath the Japanese Islands

Open Access at KIT

by Andreas Helfrich-Schkarbanenko[1], Saturo Honda[2],
Alik Ismail-Zadeh[3], Aron Sommer[1], Igor Tsepelev[4]

KIT SCIENTIFIC WORKING PAPERS 8

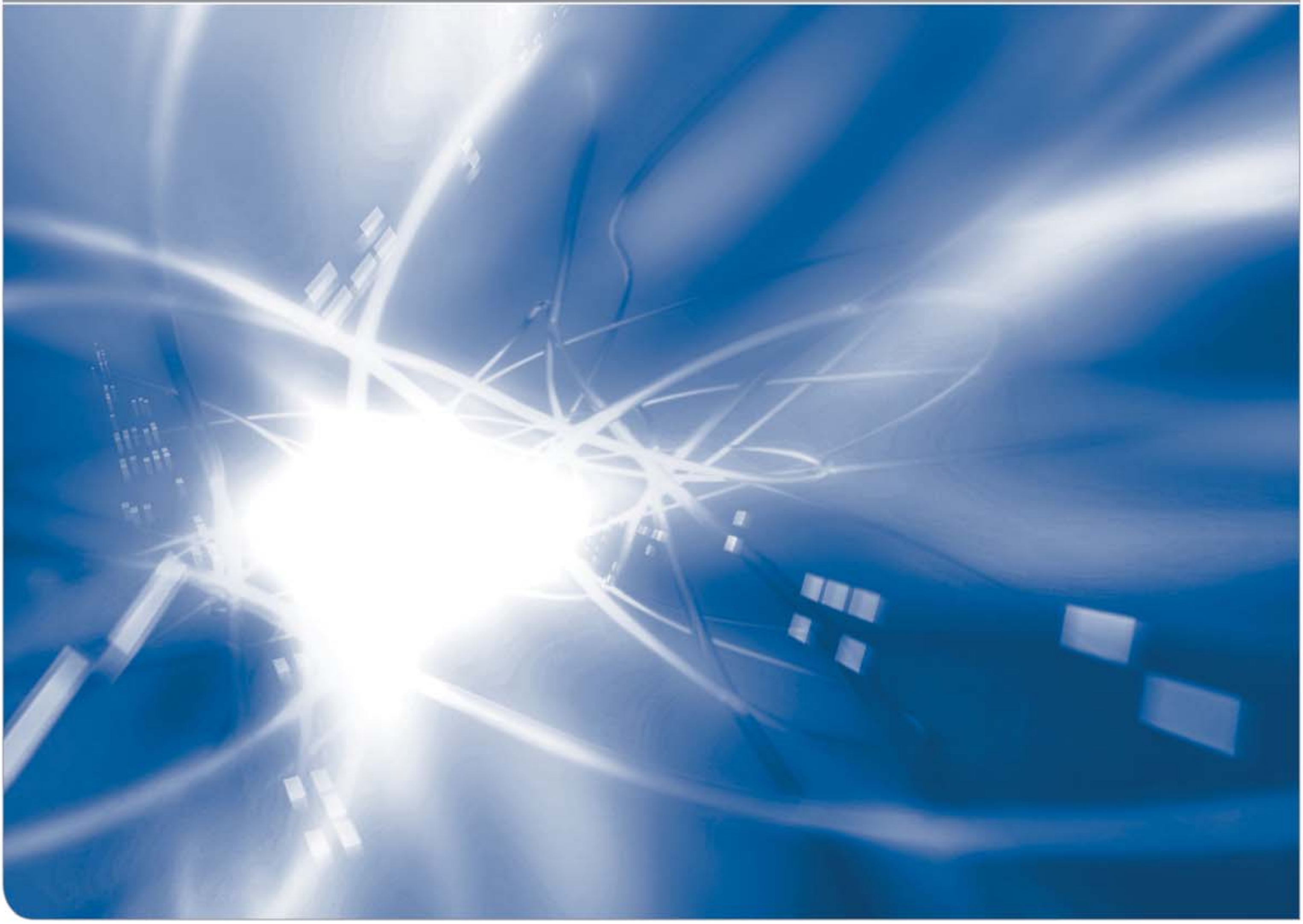

[1] Karlsruhe Institute for Technology
Institut for Applied and Numerical Mathematics 4
Karlsruhe, Germany

[2] University of Tokyo
Earthquake Research Institute
Tokyo, Japan

[3] Karlsruhe Institute of Technology
Institute of Applied Geosciences
Karlsruhe, Germany

[4] Russian Academy of Sciences
Institute of Mathematics and Mechanics
Yekaterinburg, Russia

In addition to this article we created an interactive multimedia iBook which can be downloaded at iTunesU LINK and at iBook store LINK, respectively.

A hypothesis about lithosphere subduction evolution beneath Japanese islands related to the current article is published in Ismail-Zadeh, A., Honda, S. & Tsepelev, I., Linking mantle upwelling with the lithosphere descent and the Japan Sea evolution: a hypothesis, Sci. Rep. 3,1137; DOI: 10.1038/srep01137 (2013). http://www.nature.com/srep/2013/130125/srep01137/full/srep01137.html.

This work was supported by the Deutsche ForschungsGemeinschaft (IS 203/1-1), the Chair of Petrology of KIT, the Grant-in-Aid for Scientific Research Program from the Japan Society for the Promotion of Science (JSPS 19104011), a Visiting Researcher Program from the Earthquake Research Institute of the University of Tokyo, and the Program of Basic Research of the Russian Academy of Sciences.

Karlsrue Institute of Technology
Institute for Applied and Numerical Mathematics 4
Fritz-Erler-Str. 23, Geb. 01.86
76133 Karlsruhe
http://www.math.kit.edu/ianm4/

Impressum

Karlsruher Institut für Technologie (KIT)
www.kit.edu

June 2013

ISSN: 2194-1629

VISUALIZATION OF LITHOSPHERE SUBDUCTION: APPLICATION TO THE MANTLE EVOLUTION BENEATH THE JAPANESE ISLANDS

ANDREAS HELFRICH-SCHKARBANENKO[1], SATURO HONDA[2], ALIK ISMAIL-ZADEH[3], ARON SOMMER[1], IGOR TSEPELEV[4]

ABSTRACT. In this article we illustrate how visualization of scientific data helps in interpreting results of three-dimensional (3-D) numerical modeling. We visualize the evolution of the descending lithosphere (lithosphere subduction) beneath the Japanese Islands assimilating geophysical, geodetic, and geological data. Using 3-D visualization tools we illustrate here that the hot mantle upwelling beneath the descending Pacific plate penetrated through the plate into the mantle wedge.

1. **Introduction.** Visualization assists significantly in analyzing of scientific data and in interpreting the results obtained by three-dimensional (3-D) numerical modeling of dynamics processes in the Earth interior. The purpose of scientific visualization is to enable geoscientists to illustrate, analyze, and understand these complex processes based on observations and modeling results. In this paper, we discuss the results of the evolution of lithosphere subduction and hot mantle upwelling beneath the Japanese islands and their surroundings (as presented in [8]).

The word "subduction" came from the Latin *subductus*, which means "transfer". In plate tectonics, the process in which an oceanic lithosphere (plate) descends into the Earths interior is referred to as subduction. As the lithosphere moves away from an oceanic ridge, it cools, densifies, and thickens. Once the lithosphere becomes sufficiently dense compared to the underlying mantle rocks, it bends, founders, and begins sinking into the hot mantle due to gravitational instability.

An interaction of the Pacific, Okhotsk, Eurasian, and Philippine Sea lithosphere plates with the deeper mantle around the Japanese islands (see Fig. 1), is complicated by the plate subduction [4, 5] and back-arc spreading [16], which cannot be understood by the plate kinematics only. The Pacific plate subducts under the Okhotsk and the Philippine Sea plates with the relative velocity of about 9 cm/yr and 5 cm/yr, respectively, whereas the Philippine Sea plate subducts under the Eurasian plate with the relative speed of about 5 cm/yr [3]. The lithosphere subduction results in earthquakes and volcano eruptions. For example, the 2011 Great East Japan earthquake, which caused the devastating tsunami disaster, was associated with the Pacific plate subduction. Therefore, understanding of the evolution of this plate subduction is of a major scientific interest.

A cause of the Japan Sea back-arc opening is one of scientific challenges. Seismic tomography of the mantle beneath the Japanese islands and their surroundings revealed a low velocity region. This region is believed to be of primarily thermal origin with an excess temperature of 200

Key words and phrases. lithosphere subduction, visualization, quasi-reversibility method.
[1]Karlsruhe Institute of Technology, Institute for Applied and Numerical Mathematics 4, Karlsruhe, Germany
[2]University of Tokyo, Earthquake Research Institute, Tokio, Japan
[3]Karlsruhe Institute of Technology, Institute of Applied Geosciences, Karlsruhe, Germany
[4]Russian Academy of Sciences, Institute of Mathematics and Mechanics, Yekaterinburg, Russia

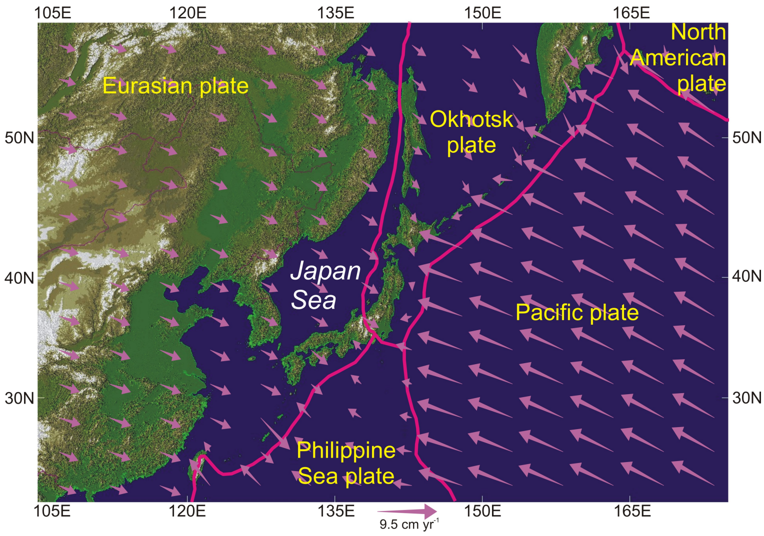

FIGURE 1. Lithospheric interaction around the Japanese Islands (modified after Ismail-Zadeh et al., [8]).

K and the associated fractional melt of less than 1%, and extends oceanward from Northern Honshu at depths of about 410 km [19]. To clarify the origin of the hot temperature anomaly beneath the Pacific plate and its implication for back-arc basin evolution, Ismail-Zadeh et al. [8] studied the mantle evolution beneath the Japanese islands and their surroundings based on assimilation of the temperature inferred from seismic tomography [4], the present movements derived from geodetic observations [3], and the past plate motion inferred from paleogeographic and paleomagnetic plate reconstructions [6, 18, 21, 24].

2. **Data assimilation.** The Earths mantle is heated from the core and from inside due to decay of radioactive elements. Since thermal convection in the mantle is described by heat advection and diffusion, one can ask: is it possible to tell, from the present temperature estimations of the mantle, something about its temperature in the geological past? Even though heat diffusion is irreversible in the physical sense, it is possible to predict accurately the heat transfer in the past without contradicting the basic thermodynamic laws.

The inverse retrospective problem of thermal convection in the mantle is an ill-posed problem, since the backward heat problem (describing both heat advection and conduction through the mantle backwards in time) possesses the properties of ill-posedness. In particular, the solution to the problem does not depend continuously on the initial data [17]. As for the existence and uniqueness of the solution to the backward heat problem, they are proven for several specific cases. The authors do not know any proven statements about existence and uniqueness of the solution either to the direct or to the inverse thermal convection problem in 3-D cases.

To restore thermal structures in the mantle (e.g., descending lithosphere or ascending mantle plumes, that is, hot mantle rocks rising through the surrounding colder rocks) in the geological past, data assimilation techniques can be used to constrain the initial conditions for the mantle temperature and velocity from their present observations. The initial conditions so obtained can then be used to run forward models of mantle dynamics to restore the evolution of mantle structures. Data assimilation can be defined as the incorporation of observations (in the present) and initial conditions (in the past) in an explicit dynamic model to provide time continuity and coupling among the physical fields (e.g., velocity, temperature). The basic principle of data assimilation is to consider the initial condition as a control variable and to optimize the initial condition in order to minimize the discrepancy between the observations and the solution of the model.

If heat diffusion is neglected, the present mantle temperature and flow can be assimilated into the past using the backward advection (e.g., [15, 22]). Both direct (forward in time) and inverse (backward in time) advection problems are well-posed. This is because the time-dependent advection equation has the same form of characteristics for the direct and inverse velocity field (the vector velocity reverses its direction, when time is reversed).

The use of the variational (VAR) data assimilation method in geodynamic modeling was pioneered by Bunge et al. [1] and Ismail-Zadeh et al. [9]. The VAR data assimilation algorithm was applied to restore numerically models of present prominent mantle plumes to their past stages [12] and to recover the structure of mantle plumes prominent in the past from that of present plumes weakened by thermal diffusion [13].

The quasi-reversibility (QRV) method was employed in geodynamic modeling by Ismail-Zadeh et al. [10] and implies the introduction into the backward heat equation of the additional term involving the product of a small regularization parameter and a higher order temperature derivative. The data assimilation in this case is based on a search of the best fit between the forecast model state and the observations by minimizing the regularization parameter. Although the QRV method is less accurate compared to the VAR method, it is more robust and requires less computational efforts. The QRV method was employed to restore the evolution of descending lithosphere beneath the southeastern Carpathian [14] and the Japanese Islands [8] regions.

Ismail-Zadeh et al. [8] reconstructed the thermal states of the mantle beneath the Japanese Islands assimilating geophysical, geodetic, and geological data up to 40 million years. Based on the results, they hypothesized that the hot mantle upwelling beneath the Pacific plate partly penetrated through breaches of the subducting plate into the mantle wedge and generated two smaller hot upwellings, which contributed to the evolution of the basins of the Japan Sea and to back-arc spreading. Also they showed that another part of the hot mantle migrated upward beneath the Pacific lithosphere, and the presently observed hot anomaly is a remnant part of this mantle upwelling.

In this article we present the model developed by Ismail-Zadeh et al. [8] and discuss the model results in the light of 3-D visualization.

3. **Mathematical description.** In the 3-D model domain

$$\overline{\Omega} = [0, x_1 = 4.000\, km] \times [0, x_2 = 4.000\, km] \times [0, x_3 = 800\, km]$$

and for time interval $t \in [0, \vartheta]$ we solve the system of regularized Stokes, the incompressibility, and the heat balance equations backward in time using the QRV method [10] and the extended Boussinesq approximation [2, 7]:

$$-\nabla P + \nabla \cdot (\eta(\nabla \boldsymbol{u} + (\nabla \boldsymbol{u})^\top)) - (\boldsymbol{E} + \varsigma\nabla^2)^{-1}(RaT - a_1 La\,\Phi_1(\pi_1) - a_2 La\,\Phi_2(\pi_2))\,\boldsymbol{e} = 0, \quad (1)$$

$$\nabla \cdot \boldsymbol{u} = 0, \quad (2)$$

$$\tfrac{\partial}{\partial t}(\boldsymbol{E} + \beta\nabla^2)^2 T - \boldsymbol{u}\cdot\nabla T - A^{-1}B\,Di^*\,Ra\,u_3\,T + A^{-1}(-\nabla^2 T + Di^*\eta\sum_{i,\,j=1}^{3} e_{ij}^2) = 0 \quad (3)$$

with appropriate boundary and initial conditions (see below). Here

$$\begin{aligned} A &= \Big[1 + \big(a_1 \tfrac{2}{w_1}(\Phi_1 - \Phi_1^2)\overline{\gamma}_1^2 + a_2 \tfrac{2}{w_2}(\Phi_2 - \Phi_2^2)\overline{\gamma}_2^2\big) Di^*\,La\,T\Big] > 0, \\ B &= \Big[1 + \tfrac{La}{Ra}\big(a_1 \tfrac{2}{w_1}(\Phi_1 - \Phi_1^2)\overline{\gamma}_1^2 + a_2 \tfrac{2}{w_2}(\Phi_2 - \Phi_2^2)\overline{\gamma}_2^2\big)\Big], \\ \Phi_i &= \tfrac{1}{2}\Big[1 + \tanh\tfrac{\pi_i}{w_i}\Big], \qquad \pi_i = z_i - x_3 - \overline{\gamma}_i(T - T_i), \qquad i = 1, 2, \end{aligned}$$

$\boldsymbol{x} = (x_1, x_2, x_3)^\top$, $\boldsymbol{u} = (u_1(x), u_2(x), u_3(x))^\top$, t, T, P and η are the dimensionless Cartesian coordinates, velocity, time, temperature, pressure, and viscosity, respectively; ϑ is the present time; $e_{ij}(\boldsymbol{u}) = \partial u_i/\partial x_j + \partial u_j/\partial x_i$ is the strain rate tensor; $\boldsymbol{e} = (0, 0, 1)^\top$ is a unit vector; ∇ is the gradient operator; and $\boldsymbol{E}$ is the unit operator. With regard to the phase changes around $x_3 = 410\,km$ and $x_3 = 660\,km$, respectively, π_1 and π_2 are the dimensionless excess pressures; and Φ_1 and Φ_2 are the phase functions describing the relative fraction of the heavier phase, respectively, and varying between 0 and 1 as a function of depth and temperature. The Rayleigh (Ra), Laplace (La), and modified dissipation (Di^*) dimensionless numbers are defined as $Ra = \alpha g \rho^* T^* h^3 (\eta^*\kappa)^{-1}$, $La = \rho^* g h^3 (\eta^*\kappa)^{-1}$, and $Di^* = \eta^*\kappa(\rho^* c h^2 T^*)^{-1}$, respectively. The operator $(\boldsymbol{E} + \varsigma\nabla^2)^{-1}$ is applied to the right-hand side of the Stokes equation (1) to smooth temperature jumps at the phase boundaries and to enhance the stability of computations. Length, temperature, and time are normalized by h, T^*, and $h^2\kappa^{-1}$, respectively. A temperature- and depth-dependent Newtonian rheology $\eta = \eta(T, x_3)$ is considered:

$$\eta(T,\, x_3) \;=\; \frac{10^{-2}\eta^*\eta_0(T,\, x_3)}{\eta_{\min}},$$

where

$$\begin{aligned} \eta_0(T,\, x_3) &= 10^{-2}\exp\Big(\frac{E_a + V_a\rho_* g x_3}{R\,T}\Big), \\ \eta_{\min} &= \min_{x_3}\eta_0(T(\boldsymbol{x}),\, x_3). \end{aligned}$$

The viscosity at $t = 0$ is shown in Fig. 2 (b). The physical parameters used in this study are listed in Table 1.

3.1. **Boundary conditions.** At the upper surface of the model boundary we prescribe the velocity of plate motion and temperature $T = T_u$. At the lower surface of the model boundary we set the velocity $\boldsymbol{u} \equiv 0$ (no-slip) and fixed temperature $T = T_1$. We prescribe at the lateral sides of the boundary $\partial\Omega$ the following homogeneous Neumann conditions:

$$\frac{\partial \boldsymbol{u}}{\partial \boldsymbol{n}} \;=\; 0, \qquad \frac{\partial T}{\partial \boldsymbol{n}} \;=\; 0,$$

where $\boldsymbol{n}$ denotes the outward normal vector at $\in \partial\Omega$. Also we prescribe $\frac{\partial P}{\partial \boldsymbol{n}} = 0$ at the model boundary.

Parameter	**Symbol**	**Value**
Dimensionless density jump at the 410-km phase boundary	a_1	0.05
Dimensionless density jump at the 660-km phase boundary	a_2	0.09
Thermal conductivity	c	1250 $W m^{-1} K^{-1}$
Activation energy	E_a	$3 \cdot 10^5$ $J\, mol^{-1}$
Acceleration due to gravity	g	9.8 $m\, s^{-2}$
Depth	h	800 km
Length (in x-direction)	l_1	4000 km
Length (in y-direction)	l_2	4000 km
Universal gas constant	R	8.3144 $J\, mol^{-1} K^{-1}$
Difference between the temperatures at the lower (T_l) and upper (T_u) model boundaries	T^*	1594 K
Dimensionless temperature at the upper model boundary	T_u	$290\, K\, /\, T^*$
Dimensionless temperature at the lower model boundary	T_l	$1884\, K\, /\, T^*$
Dimensionless temperature at the 410-km phase boundary	T_1	$1790\, K\, /\, T^*$
Dimensionless temperature at the 660-km phase boundary	T_2	$1891\, K\, /\, T^*$
Activation volume	V_a	$4 \cdot 10^{-6}$ $m^3\, mol^{-1}$
Dimensionless width of the 410-km phase transition	w_1	10 $km\, /\, h$
Dimensionless width of the 660-km phase transition	w_2	10 $km\, /\, h$
Dimensionless depth of the 410-km phase boundary	z_1	390 $km\, /\, h$
Dimensionless depth of the 660-km phase boundary	z_2	140 $km\, /\, h$
Thermal expansivity	α	$3 \cdot 10^{-5}$ K^{-1}
QRV regularization parameter	β	0.00001
Dimensionless Clapeyron (pressure-temperature) slope at the 410-km phase boundary 1	$\overline{\gamma}_1$	$4 \cdot 10^6$ $Pa\, K^{-1}$ $T^* (\rho^* g h)^{-1}$
Dimensionless Clapeyron slope at the 660-km phase boundary 2	$\overline{\gamma}_2$	$-2 \cdot 10^6$ $Pa\, K^{-1}$ $T^* (\rho^* g h)^{-1}$
Reference viscosity	η^*	10^{21} $Pa\, s$
Thermal diffusivity	κ	10^{-6} $m^2\, s^{-1}$
Reference density	ρ^*	3400 $kg\, m^{-1}$
Phase regularization parameter	ς	0.0001

TABLE 1. Model parameters.

3.2. **Initial conditions.** The present temperature model beneath the Japanese Islands is developed by using the high-resolution seismic tomography (P-wave velocity anomalies) for the region [19]. The temperature anomalies (Fig. 2 (a)) are inferred from the seismic wave anomalies using a non-linear inversion method and considering the effects of mantle composition, anelasticity, and partial melting on seismic velocities (as described by Ismail-Zadeh et al., [11]). The temperature anomalies are then added to the vertical temperature profile to obtain the present temperature model. At shallow depth (down to 110 km), the solution of the cooling half-space model with 48 million years after the start of cooling is used. At deeper level, the adiabatic temperature distribution with the potential temperature of 1330°C is employed. The crustal temperature is calculated by estimating the geothermal gradient from measured regional surface heat flow. The temperature model so obtained is used as the initial condition for restoration (inverse retrospective) models.

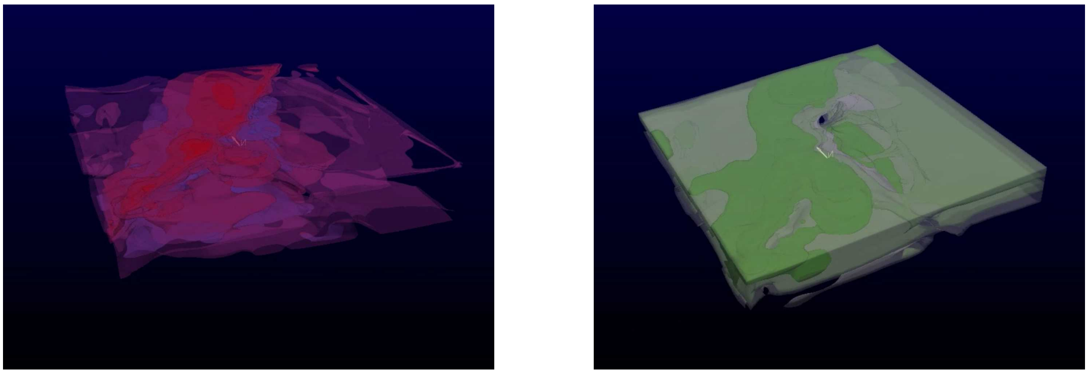

(a) (b)

FIGURE 2. 3-D dynamic visualization of the initial temperature anomaly dT (a) and initial viscosity η (b), illustrated by isosurfaces.

4. **Numerical solvers.** The governing equations with the prescribed boundary and initial conditions are solved numerically by the finite-volume method [7].

- $\boldsymbol{u}$ and P are found from the equation (1) and (2) using the SIMPLE method [7].
- The regularized heat balance equation (3) is approximated by Euler method using the implicit approximation $C = -C^\top$ of the advective term and the explicit approximation $D = D^\top$ of the conductive term:

$$(E + \beta D)^2 \frac{T^{k+1} - T^k}{dt} + CT^{k+1} - DT^k + f(u, T^k) \ = \ 0.$$

- To solve the numerical scheme we use the splitting method [20] introducing the convection/antidiffusion and regularization parts as

$$(E + dt\, C)T^{k+1/2} \ = \ (E + dt\, D)t^k - dt\, f(u, T^k), \tag{4}$$

$$(E + \beta D)^2 T^{k+1} \ = \ T^{k+1/2}. \tag{5}$$

- The system (4) is solved by the BiConjugate Gradient method [23] using the incomplete LU-factorization as a pre-conditioner.
- The system (5) is solved by conjugate gradient method [7].

5. **Results of visualization and scientific interpretation.** High-temperature patchy anomaly beneath the back-arc Japan Sea basin splits into two prominent anomalies showing two small-scale upwellings beneath the southwestern (upwelling A) and northern (upwelling B) part of the Japan Sea (Fig. 3). The temperature anomalies dT are shown in Fig. 3 by iso-surfaces, where red and blue colors illustrate anomalies of 0.04 and -0.04 for upwelling A and 0.035 and -0.035 for upwelling B, respectively. The velocity field is presented by gray arrows, and the big arrow marked by N is directed northwards. The upwellings are likely to be generated in the sub-slab hot mantle and penetrated through breaches/tears of the subducting Pacific plate into the mantle wedge. Ismail-Zadeh et al. [8] propose that the present hot anomalies in the back-arc and sub-slab mantle had a single origin located in the sub-lithospheric mantle. The 3-D visualization of the model results show that upwelling B was linked to the sub-slab mantle at 40 Ma. Meanwhile upwelling A does not show the feature at the time. We may interpret this, as upwelling A penetrated via the slab into the mantle wedge earlier than upwelling B did.

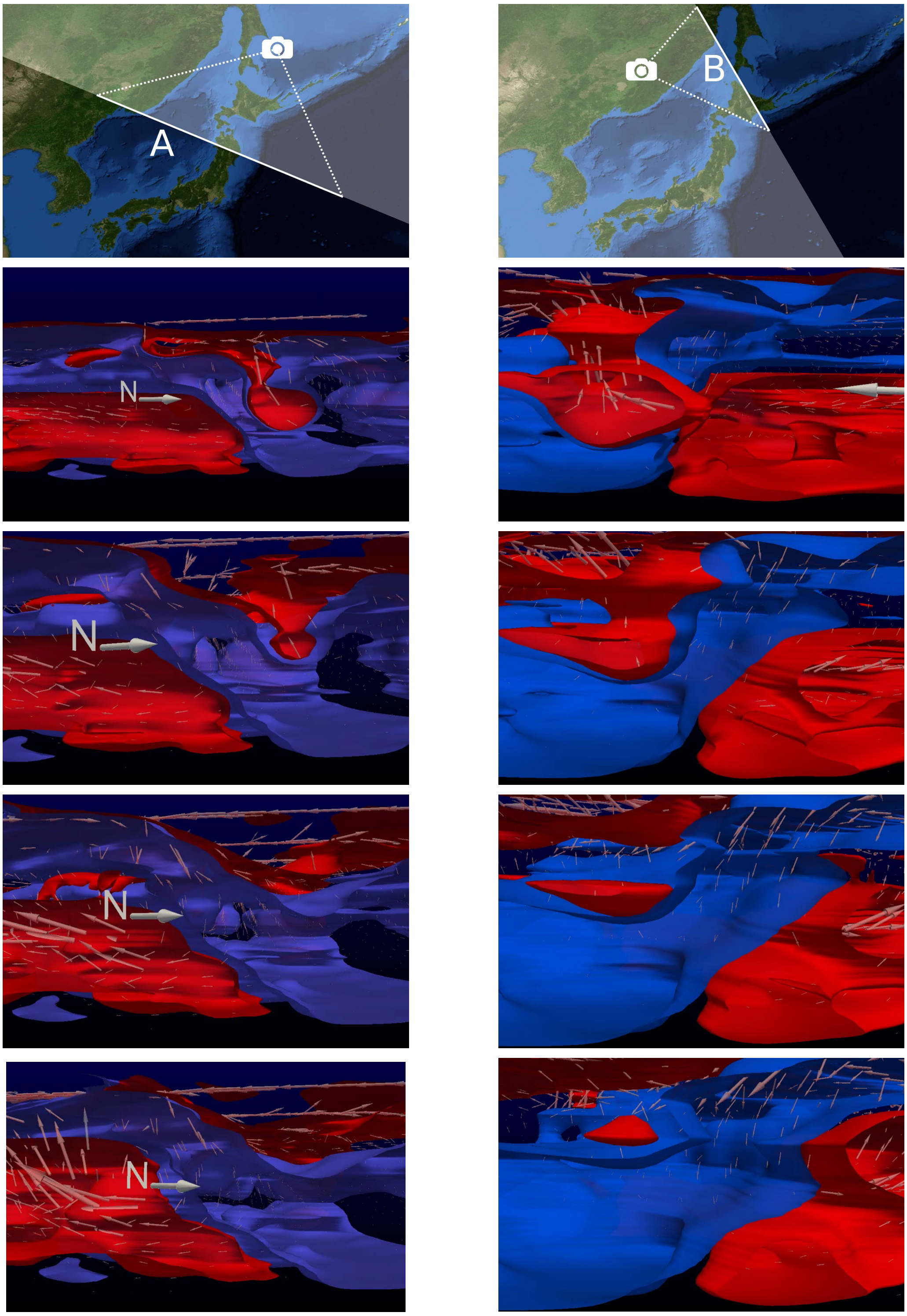

FIGURE 3. Evolution of upwelling A (left) and upwelling B (right) for 38.9 Ma, 29.18 Ma, 19.45 Ma, and present (from the top to the down, respectively). Surface topography map produced by Reto Stöckli, Blue Marble: Next Generation on the NASA Earth Observatory.

6. **Conclusions.** It is known that the opening of the Japan Sea has temporal and spatial variations and shows several stages of deformation. Inhomogeneous spreading is consistent with the patchy character of hot materials as evident in our results. Non-instantaneous deformation may imply that the hot materials have penetrated through, or affected, the overlying subducting Pacific lithosphere several times. The tomography images of a subducting slab usually do not show a single straight high velocity anomaly as one may expect from the forward numerical simulations of subducting lithosphere. Instead they appear to show a couple of high velocity blocks. Such a feature may be explained by an occasional penetration of hot materials below the subducting lithosphere.

7. **Acknowledgments.** This work was supported by the Deutsche ForschungsGemeinschaft (IS 203/1-1), the Grant-in-Aid for Scientific Research Program from the Japan Society for the Promotion of Science (JSPS 19104011), a Visiting Researcher Program from the Earthquake Research Institute of the University of Tokyo, and the Program of Basic Research of the Russian Academy of Sciences.

8. **Author contributions.** Satoru Honda and Alik Ismail-Zadeh contributed equally to scientific idea development, design of the numerical experiments, analysis of the data and geodynamic interpretation of numerical results. Igor Tsepelev developed a numerical code, Igor Tsepelev and Alik Ismail-Zadeh carried out numerical experiments. Andreas Helfrich- Schkarbanenko and Aron Sommer visualized the results and developed movies. They together with Alik Ismail-Zadeh build the interactive iBook and wrote the paper.

REFERENCES

[1] Bunge, H. P, Hagelberg, C. R. & Travis, B. J. Mantle circulation models with variational data assimilation: Inferring past mantle flow and structure from plate motion histories and seismic tomography. Geophys. J. Int. 152, 280-301 (2003).

[2] Christensen, U. R. & Yuen, D. A. Layered convection induced by phase transitions. J. Geophys. Res. 90, 10291-10300 (1985).

[3] Drewes, H. The Actual Plate Kinematic and Crustal Deformation Model APKIM2005 as basis for a non-rotating ITRF, In: Geodetic Reference Frames, H. Drewes (Ed.), IAG Symposia series, 134, 95-99, Springer, Berlin (2009).

[4] Fukao, Y., Widiyantoro, S. & Obayashi, M. Stagnant slabs in the upper and lower mantle transition region. Rev. Geophys. 39, 291-323 (2001).

[5] Furumura, T. & Kennett, B. L. N. Subduction zone guided waves and the heterogeneity structure of the subducted plate intensity anomalies in northern Japan. J. Geophys. Res. 110, B10302, doi: 10.1029/2004JB003486 (2005).

[6] Hall, R. Cenozoic geological and plate tectonic evolution of SE Asia and the SW Pacific: computer based reconstructions, model and animations. J. Asia Earth Sci. 20, 353-431 (2002).

[7] Ismail-Zadeh, A. & Tackley, P. Computational Methods for Geodynamics. Cambridge University Press, Cambridge (2010).

[8] Ismail-Zadeh, A., Honda, S. & Tsepelev, I., Linking mantle upwelling with the lithosphere descent and the Japan Sea evolution: a hypothesis, Sci. Rep. 3,1137; DOI: 10.1038/srep01137 (2013).

[9] Ismail-Zadeh, A. T, Korotkii, A. I., Naimark, B. M. & Tsepelev, I. A. Three-dimensional numerical simulation of the inverse problem of thermal convection. Comput. Math. and Mathem. Phys. 43, 587-599 (2003).

[10] Ismail-Zadeh, A., Korotkii, A., Schubert, G. & Tsepelev, I. Quasi-reversibility method for data assimilation in models of mantle dynamics. Geophys. J. Int. 170, 1381-1398 (2007).

[11] Ismail-Zadeh, A., Mueller, B. & Schubert, G. Three-dimensional modeling of present-day tectonic stress beneath the earthquake-prone southeastern Carpathians based on integrated analysis of seismic, heat flow, and gravity observations. Phys. Earth Planet. Inter., 149, 81-98 (2005).

[12] Ismail-Zadeh, A., Schubert, G., Tsepelev, I. & Korotkii, A. Inverse problem of thermal convection: Numerical approach and application to mantle plume restoration. Phys. Earth Planet. Inter. 145, 99-114 (2004).

[13] Ismail-Zadeh, A., Schubert, G., Tsepelev, I. & Korotkii, A. Three-dimensional forward and backward numerical modeling of mantle plume evolution: Effects of thermal diffusion. J. Geophys. Res. 111, B06401, doi:10.1029/2005JB003782 (2006).

[14] Ismail-Zadeh, A., Schubert, G., Tsepelev, I. & Korotkii, A. Thermal evolution and geometry of the descending lithosphere beneath the SE-Carpathians: An insight from the past. Earth Planet. Sci. Lett. 273, 68-79 (2008).
[15] Ismail-Zadeh, A. T., Tsepelev, I. A., Talbot, C. J. & Korotkii, A. I. Three-dimensional forward and backward modelling of diapirism: Numerical approach and its applicability to the evolution of salt structures in the Pricaspian basin. Tectonophysics 387, 81-103 (2004).
[16] Jolivet, L., Tamaki, K. & Fournier, M. Japan Sea, opening history and mechanism: A synthesis. J. Geophys. Res. 99, 22232-22259 (1994).
[17] Kirsch, A. An Introduction to the Mathematical Theory of Inverse Problems. Springer-Verlag, New York, 1996.
[18] Northrup, C. J., Royden, L. H. & Burchfiel, B. C. Motion of the Pacific plate relative to Eurasia and its potential relation to Cenozoic extension along the eastern margin of Eurasia. Geology 23, 719-722 (1995).
[19] Obayashi, M., Sugioka, H., Yoshimitsu, J. & Fukao, Y. High temperature anomalies oceanward of subducting slabs at the 410-km discontinuity. Earth Planet. Sci. Lett. 243, 149-158 (2006).
[20] Samarski, A. A., Vabischevich, P. N. Computational Heat Transfer. Vol 1. Mathematical Modeling. John Wiley & Sons, New York (1995).
[21] Seno, T. & Maruyama, S. Paleogeographic reconstruction and origin of the Philippine Sea. Tectonophysics 102, 53-84 (1984).
[22] Steinberger, B. & OConnell, R. J. Advection of plumes in mantle flow: implications for hotspot motion, mantle viscosity and plume distribution. Geophys. J. Int. 132, 412-434 (1998).
[23] Van der Vorst, H. A. Bi-CGSTAB: A fast and smoothly converging variant of BiCG for the solution of nonsymmetric linear systems, SIAM J. Sci. Stat. Comp. 13, 631-644, (1992).
[24] Yamazaki, T., Takahashi, M., Iryu, Y., Sato, T., Oda, M., Takayanagi, H., Chiyonobu, S., Nishimura, A., Nakazawa, T. & Ooka, T. Philippine Sea Plate motion since the Eocene estimated from paleomagnetism of seafloor drill cores and gravity cores. Earth Planet Space 62, 495-502 (2010).

KIT Scientific Working Papers
ISSN 2194-1629
www.kit.edu